PROCEEDINGS OF SCIENCE

Non-Perturbative Renormalization for Staggered Fermions (Self-energy Analysis)

Jangho Kim*, **Boram Yoon, and Weonjong Lee**
Lattice Gauge Theory Research Center, CTP, and FPRD,
Department of Physics and Astronomy,
Seoul National University, Seoul, 151-747, South Korea
E-mail: wlee@snu.ac.kr

SWME Collaboration

We present preliminary results of data analysis for the non-perturbative renormalization (NPR) on the self-energy of the quark propagators calculated using HYP improved staggered fermions on the MILC asqtad lattices. We use the momentum source to generate the quark propagators. In principle, using the vector projection operator of $(\overline{\overline{\gamma_\mu \otimes 1}})$ and the scalar projection operator $(\overline{\overline{1 \otimes 1}})$, we should be able to obtain the wave function renormalization factor Z_q' and the mass renormalization factor $Z_q \cdot Z_m$. Using the MILC coarse lattice, we obtain a preliminary but reasonable estimate of Z_q' and $Z_q \cdot Z_m$ from the data analysis on the self-energy.

The 30th International Symposium on Lattice Field Theory - Lattice 2012
June 24-29, 2012
Cairns Convention Centre, Cairns, Australia

*Speaker.

PoS(Lattice 2012)241

1. Introduction

We can obtain the wave function renormalization factor Z'_q defined in the RI′-MOM scheme and the mass renormalization factor $Z_q \cdot Z_m$ defined in the RI-MOM scheme from the staggered quark propagator using non-perturbative renormalization (NPR) method. We generate the staggered quark propagators using the momentum source in the Landau gauge on the MILC coarse lattices [1, 2]. Here, we present results of the data analysis after the projection.

2. Mass Renormalization

Let us consider a staggered fermion propagator.

$$S^f_{cc'}(x_1,x_2) \equiv \langle \chi^f_c(x_1)\overline{\chi}^f_{c'}(x_2)\rangle\,, \tag{2.1}$$

where f is a flavor index, c, c' are color indices. Here, x_1 and x_2 represent the position coordinates on the lattice with $x_1, x_2 \in \mathbb{Z}^4$. The lattice spacing is a.

In the normal Brillouin zone, we use p, q as the momentum, and, in the reduced Brillouin zone, we use $\tilde{p}$, $\tilde{q}$ as the momentum as follows,

$$p,q \in (-\frac{\pi}{a},\frac{\pi}{a}]^4\,, \qquad \tilde{p},\tilde{q} \in (-\frac{\pi}{2a},\frac{\pi}{2a}]^4\,, \qquad q = \tilde{q}+\pi_A\,, \qquad p = \tilde{p}+\pi_B\,, \tag{2.2}$$

where A, B are hypercubic vectors whose element is 0 or 1, and $\pi_A \equiv \dfrac{\pi}{a}A$.

The staggered quark propagator is defined as

$$\hat{S}^f_{cc'}(\tilde{p}+\pi_A,\tilde{q}+\pi_B) \equiv \langle \widetilde{\chi}^f_c(\tilde{p}+\pi_A)\widetilde{\overline{\chi}}^f_{c'}(\tilde{q}+\pi_B)\rangle\,. \tag{2.3}$$

Using the Fourier analysis, one can show the following relationship.

$$\hat{S}^f_{cc'}(\tilde{p}+\pi_A,\tilde{q}+\pi_B) = \widetilde{\delta}^{(4)}(\tilde{p}-\tilde{q})[\widetilde{S}(\tilde{p})]^f_{AB;cc'} \tag{2.4}$$

where

$$\widetilde{\delta}^{(4)}(\tilde{p}) \equiv (2a)^4 \sum_{y\in\mathbb{W}^4} e^{i\tilde{p}y} \tag{2.5}$$

Here, y represents a position coordinate of a hypercube whose lattice spacing is $2a$, $y \in \mathbb{W}^4$, and $\mathbb{W}$ denotes one-dimensional lattice whose spacing is $2a$. By setting $\tilde{p} = \tilde{q}$, the quark propagator becomes

$$\hat{S}^f_{cc'}(\tilde{p}+\pi_A,\tilde{p}+\pi_B) = \widetilde{\delta}^{(4)}(0)[\widetilde{S}(\tilde{p})]^f_{AB;cc'} = V[\widetilde{S}(\tilde{p})]^f_{AB;cc'}\,, \tag{2.6}$$

where V is lattice volume factor.

$$V \equiv (2a)^4 \sum_{y\in\mathbb{W}^4} 1 = L^3 \times T \tag{2.7}$$

where L (T) is lattice size in the spacial (time) direction.

PoS(Lattice 2012)241

To obtain the propagator, we have to solve the staggered Dirac equation.

$$\begin{aligned}(\not{D}_s + m^f)_i \psi_i^f &= h \\ \psi_i^f &= \frac{1}{(\not{D}_s + m^f)_i} h,\end{aligned} \tag{2.8}$$

where i is a gauge configuration index, $(\not{D}_s + m^f)_i$ is Dirac operator for staggered fermion. h is a source vector, and ψ_i^f is a solution vector of the Dirac equation for a specific gauge configuration i.

$$S_i^f(x_1, x_2) = \frac{1}{(\not{D}_s + m^f)_i} \tag{2.9}$$

where $S_i^f(x_1,x_2)$ is a propagator for a specific gauge configuration i. A thermalized quark propagator is defined as

$$S^f_{cc'}(x_1, x_2) = \frac{1}{N} \sum_i^N S^f_{i;cc'}(x_1, x_2), \tag{2.10}$$

where N is the number of gauge configurations.

S^f and S_i^f are quite different. S_i^f do not conserve the momentum, because there are external gluons which live for a short time in a Monte Carlo evolution time. But S^f conserve the momentum in the reduced Brillouin zone. The difference is shown in Figure 1.

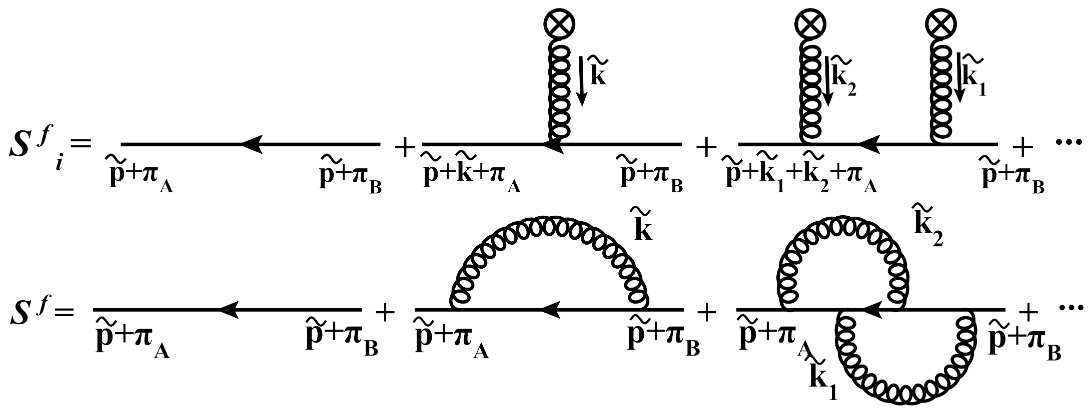

Figure 1: S_i^f has temporal external gluons, while all the gluons are contracted in S^f.

The solution vector ψ_i^f is

$$\psi^f_{i;a}(x_1) = a^4 \sum_{x_2 \in \mathbb{Z}^4} S^f_{i;ab}(x_1, x_2) h_b(x_2) \tag{2.11}$$

We set the source vector $h_b(x_2, \tilde{p} + \pi_B) = e^{-i(\tilde{p}+\pi_B)x_2} \delta_{bc}$.

$$\psi^f_{i,ac}(x_1, \tilde{p} + \pi_B) = a^4 \sum_{x_2 \in \mathbb{Z}^4} S^f_{i;ab}(x_1, x_2) e^{-i(\tilde{p}+\pi_B)x_2} \delta_{bc} \tag{2.12}$$

After we calculate $\psi^f_{i;ac}(x_1,\tilde{p}+\pi_B)$ using conjugate gradient method for each c, we can obtain the full matrix of $\psi^f_{i;ab}(x_1,\tilde{p}+\pi_B)$:

$$\hat{S}^f_{ab}(\tilde{p}+\pi_A,\tilde{p}+\pi_B) = \frac{a^4}{N}\sum_i^N \sum_{x_1\in\mathbb{Z}^4} e^{i(\tilde{p}+\pi_A)x_1}\psi^f_{i;ab}(x_1,\tilde{p}+\pi_B) = V[\widetilde{S}(\tilde{p})]^f_{AB;ab} \tag{2.13}$$

The inverse bare propagator can be expressed as follows,

$$\begin{aligned}[\widetilde{S}^f(\tilde{p})]^{-1}_{AB;cc'} = [(1+\Sigma_S)m_0^f\overline{\overline{(1\otimes 1)}}_{AB} + (1+\Sigma_V)\sum_\mu \frac{i}{a}\sin(\tilde{p}_\mu a)\overline{\overline{(\gamma_\mu\otimes 1)}}_{AB} \\ +\Sigma_T m_0^f \sum_{\mu\neq\nu}\sin(\tilde{p}_\mu a)(\sin(\tilde{p}_\nu a))^3\overline{\overline{(\gamma_{\mu\nu}\otimes 1)}}_{AB} \\ +\Sigma_A \sum_{\mu\neq\nu\neq\rho}\frac{i}{a}\sin(\tilde{p}_\mu a)(\sin(\tilde{p}_\nu a))^3(\sin(\tilde{p}_\rho a))^5\overline{\overline{(\gamma_{\mu\nu\rho}\otimes 1)}}_{AB} \\ +\Sigma_P m_0^f \sum_{\mu\neq\nu\neq\rho\neq\sigma}\sin(\tilde{p}_\mu a)(\sin(\tilde{p}_\nu a))^3(\sin(\tilde{p}_\rho a))^5(\sin(\tilde{p}_\sigma a))^7\overline{\overline{(\gamma_{\mu\nu\rho\sigma}\otimes 1)}}_{AB}]_{cc'}\end{aligned}$$

which is derived from the lattice symmetry [3]. The definition of $\overline{\overline{(\gamma_S\otimes\xi_F)}}_{AB}$ is given as

$$\begin{aligned}\overline{(\gamma_S\otimes\xi_F)}_{AB} &\equiv \frac{1}{4}Tr[\gamma_A^\dagger\gamma_S\gamma_B\gamma_F^\dagger] \\ \overline{\overline{(\gamma_S\otimes\xi_F)}}_{AB} &\equiv \frac{1}{16}\sum_{C,D}(-1)^{A\cdot C}\overline{(\gamma_S\otimes\xi_F)}_{CD}(-1)^{D\cdot B}\end{aligned} \tag{2.14}$$

The renormalization of propagator is $\widetilde{S}^f_R(p) = Z_q\widetilde{S}^f_0(p)$, and the mass renormalization is defined by $m_R = Z_m m_0$. Here, Z_q is wave function renormalization factor for quark field, Z_m is mass renormalization factor, m_R is renormalized quark mass, m_0 is a bare quark mass and the subscript R denotes a renormalized quantity, the subscript 0 denotes a bare quantity. Unless specified, we use the convention of $m = m_0$ in this paper.

The RI′-MOM scheme prescription is

$$Z'_q = -i\frac{1}{48}\sum_\mu \frac{\hat{p}_\mu}{\hat{p}^2}\mathrm{Tr}[(\overline{\overline{\gamma_\mu\otimes 1}})S^{-1}(\tilde{p})] \tag{2.15}$$

$$Z'_q\left[Z_m m + C_1\frac{\langle\bar{\chi}\chi\rangle}{\hat{p}^2}\right] = \frac{1}{48}\mathrm{Tr}[(\overline{\overline{1\otimes 1}})S^{-1}(\tilde{p})], \tag{2.16}$$

where $\hat{p}_\mu \equiv \sin(a\tilde{p}_\mu)$ and $\hat{p}^2 \equiv \sum_\mu \hat{p}_\mu^2$. So the renormalized propagator can be rewritten as

$$\widetilde{S}^f_R(p) = \frac{Z_q}{(1+\Sigma_V)}\left(\sum_\mu \frac{i}{a}\sin(\tilde{p}_\mu a)\overline{\overline{(\gamma_\mu\otimes 1)}}_{AB} + \frac{(1+\Sigma_S)}{(1+\Sigma_V)}\frac{m_R}{Z_m}\overline{\overline{(1\otimes 1)}}_{AB} + \cdots\right)^{-1} \tag{2.17}$$

Thus, we can write the Z_q and Z_m as follows,

$$Z_q = (1+\Sigma_V), \qquad Z_m = \frac{(1+\Sigma_S)}{(1+\Sigma_V)}. \tag{2.18}$$

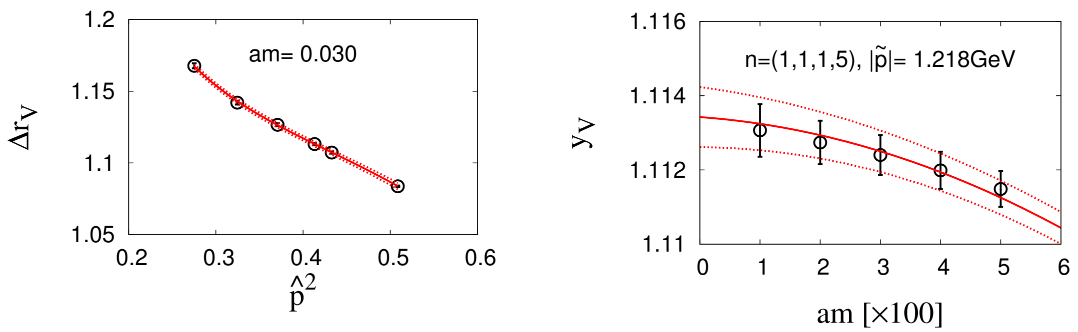

(a) Δr_V (b) y_V

Figure 2: Δr_V vs. $\hat{p}^2$ (left) and y_V vs. am (right).

3. Results

We generate staggered fermion propagators for 5 quark masses and 6 external momenta with $0.5 < |a\tilde{p}| < 0.75$. $am = 0.01, 0.02, 0.03, 0.04, 0.05$. The fitting function suggested in Ref. [4, 5, 6, 7] is

$$y_i = \frac{1}{N}\mathrm{Tr}[S^{-1}(\tilde{p})\,\mathbb{P}_i] \tag{3.1}$$

$$f_q(m,a,\hat{p}) = c_1\left(1+\Gamma_1[\log(\hat{p}^2)+2\frac{(am)^2}{\hat{p}^2}]\right)+c_2\log(\hat{p}^2)+c_3[\log(\hat{p}^2)]^2+c_4\frac{(am)^2}{\hat{p}^2} \tag{3.2}$$

$$+c_5\frac{(am)^2}{\hat{p}^2}\log(\hat{p}^2)+c_6(am)+c_7\hat{p}^2+c_8(\hat{p}^2)^2+c_9\hat{p}^4 \tag{3.3}$$

$$f_m(m,a,\hat{p}) = \frac{d_1}{\hat{p}^2}+(am)\Bigg(d_2(1+\Gamma_2[\log(\hat{p}^2)+\frac{(am)^2}{\hat{p}^2}+\frac{(am)^2}{\hat{p}^2}\log(1+\frac{\hat{p}^2}{(am)^2})]) \tag{3.4}$$

$$+d_3\log(\hat{p}^2)+d_4[\log(\hat{p}^2)]^2+d_5\frac{(am)^2}{\hat{p}^2}+d_6\frac{(am)^2}{\hat{p}^2}\log(\hat{p}^2) \tag{3.5}$$

$$+d_7\hat{p}^2+d_8(\hat{p}^2)^2+d_9\hat{p}^4\Bigg) \tag{3.6}$$

where the anomalous dimension Γ_i is

$$\Gamma_1 = -\frac{\alpha_s}{(4\pi)}\cdot\frac{4}{3}, \qquad \Gamma_2 = -\frac{\alpha_s}{4\pi}\cdot\frac{16}{3}. \tag{3.7}$$

Here, y_i represents a data point obtained by some projection $\mathbb{P}_i$.

Let us consider a data analysis for Z'_q with a vector projection: $\mathbb{P}_V = \overline{\overline{(\gamma_\mu \otimes 1)}}\hat{p}/\hat{p}^2$. We use the uncorrelated Bayesian method to fit the data to $f_q(X)$ by imposing the following prior condition: $c_1 = 1 \pm 0.5\alpha_s$, $c_{2-5} = 0 \pm 2\alpha_s^2$, and $c_{6-9} = 0 \pm 2$. Here, X represents $m, \hat{p}, a$ collectively Here, note that the prior information on c_{1-5} comes from the lattice perturbation theory [4]. In order to investigate the fitting quality, let us define Δr_V as $\Delta r_V \equiv y_V - c_9\hat{p}^4$. In Fig. 2(a) and 2(b), we present Δr_V and y_V, respectively. The fitting results are given in Table 1. As you can see in the plots, the fitting quality is quite good.

PoS(Lattice 2012)241

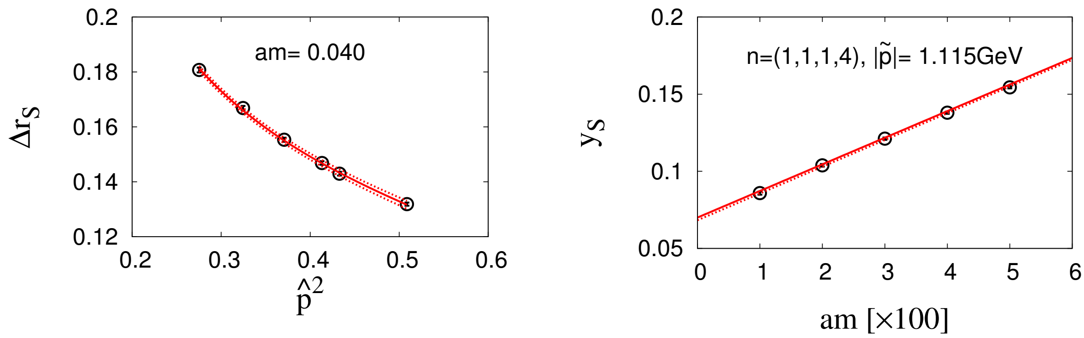

(a) Δr_S (b) y_S

Figure 3: Δr_S vs. $\hat{p}^2$ (left), and y_S vs. am (right).

Let us turn to the data analysis for the scalar projection: $\mathbb{P}_S = (\overline{\overline{1 \otimes 1}})$. We use the Bayesian method to fit the data to $f_m(X)$. The prior conditions are $d_2 = 1 \pm 0.5\alpha_s$, $d_{3-6} = 0 \pm 2\alpha_s^2$, and $d_{7-9} = 0 \pm 2$. Let us define Δr_S as $\Delta r_S \equiv y_S - d_9(am)\hat{p}^4$. In Fig. 3, we show Δr_S and y_S. As one can see in the plots, the fitting quality is somewhat poor with $\chi^2/\text{d.o.f} = 1.24(39)$ for the uncorrelated Bayesian fitting. The fitting results are summarized in Table 2.

In Fig. 4, we define the y-axis variables as

$$Z'_q(\tilde{p}) \equiv f_q(\tilde{p}; m = 0, c_{7-9} = 0) \tag{3.8}$$

$$Z_q \cdot Z_m(\tilde{p}) \equiv \frac{1}{am} f_m(\tilde{p}; m = 0, d_1 = 0, d_{7-9} = 0) \tag{3.9}$$

We estimate the statistical errors using the jackknife resampling method. As you can see in the plots, the minimum of statistical errors is located at $|\tilde{p}| = 2.084\text{GeV}$ for Z'_q and at $|\tilde{p}| = 2.190\text{GeV}$ for $Z_q \cdot Z_m$. Hence, we choose $|\tilde{p}| = 2\,\text{GeV}$ as our optimal matching scale. Our preliminary results are

$$Z'_q(\tilde{p} = 2\,\text{GeV}) = 0.9810(46)\,, \qquad Z_q \cdot Z_m(\tilde{p} = 2\,\text{GeV}) = 1.0551(52)\,. \tag{3.10}$$

Table 1: Fitting results for Z'_q.

c_1	c_2	c_3	c_4	c_5
0.931(18)	0.185(47)	0.161(28)	-0.096(18)	0.263(39)
c_6	c_7	c_8	c_9	$\chi^2/\text{d.o.f}$
-0.012(13)	0.97(17)	-1.17(19)	0.373(27)	0.35(11)

Table 2: Fitting results for $Z_q \cdot Z_m$.

c_1	c_2	c_3	c_4	c_5
0.02992(38)	1.143(11)	-0.205(19)	-0.117(20)	-0.0346(82)
c_6	c_7	c_8	c_9	$\chi^2/\text{d.o.f}$
0.0414(98)	2.358(82)	-2.66(16)	-2.55(39)	1.24(39)

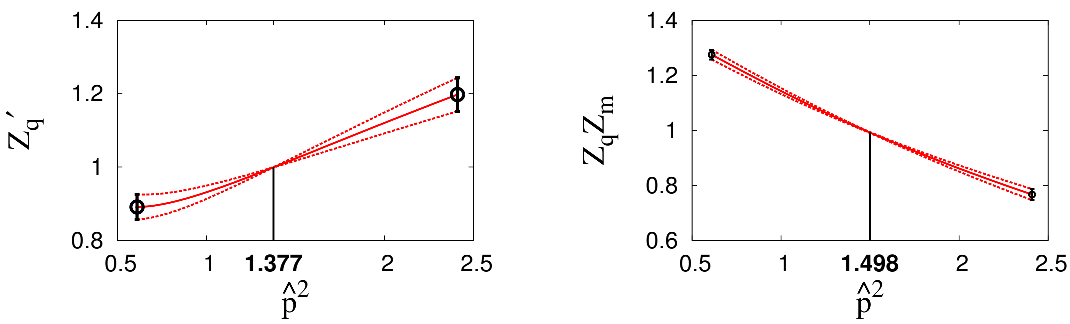

(a) Z_q' (b) $Z_q \cdot Z_m$

Figure 4: Z_q' (left) and $Z_q \cdot Z_m$ (right) as a function of $\hat{p}^2$. The solid curve represents the central value and the dotted curves represent the statistical error.

We plan to cross-check these results against those obtained using the bilinear operators in near future.

4. Acknowledgments

W. Lee is supported by the Creative Research Initiatives program (2012-0000241) of the NRF grant funded by the Korean government (MEST). W. Lee acknowledges support from the KISTI supercomputing center through the strategic support program [No. KSC-2011-G2-06]. Computations were carried out in part on QCDOC computing facilities of the USQCD Collaboration at Brookhaven National Lab, on GPU computing facilities at Jefferson Lab, on the DAVID GPU clusters at Seoul National University, and on the KISTI supercomputers. The USQCD Collaboration are funded by the Office of Science of the U.S. Department of Energy.

References

[1] Andrew T. Lytle, PoS (Lattice 2009) 202; [`arXiv:0910.3721`].

[2] Andrew T. Lytle and Stephen R. Sharpe, PoS (Lattice 2011) 237; [`arXiv:1110.5494`].

[3] Stephen R. Sharpe, private communication.

[4] Weonjong Lee, Phys. Rev. D**49**, (1994), 3563-3573; [`arXiv:hep-lat/9310018`].

[5] H. D. Politzer, Nucl. Phys. B**117**, 397 (1976).

[6] T. Blum, *et al.*, Phys. Rev. D**66**, (2002), 014504; [`arXiv:hep-lat/0102005v1`].

[7] Y. Aoki, *et al.*, RBC and UKQCD Collaboration, Phys. Rev. D**78**, (2008), 054510; [`arXiv:hep-lat/0712.1067v1`].